Heliyon 10 (2024) e39481

Contents lists available at ScienceDirect

Heliyon

journal homepage: www.cell.com/heliyon

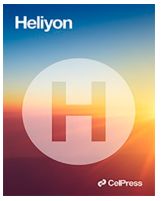

Research article

YTHDF1 gene inhibits epilepsy progression by epigenetic activation of PTEN gene

Mingxia Li [a,1], Junli Yang [b,1], Lixiang Gao [b,*]

[a] Department of Paediatrics, Yantaishan Hospital, Yantai, Shandong, 264001, China
[b] Department of Neurology, Yantai Affiliated Hospital of Binzhou Medical University, Yantai, Shandong, 264100, China

ARTICLE INFO

Keywords:
Epilepsy
YTHDF1 gene
PTEN gene
Epigenetic

ABSTRACT

Epilepsy is a common chronic neurological disorder with high prevalence that profoundly affects millions of people worldwide. Inflammatory dysregulation affects central nervous system disorders including epilepsy, and YTHDF1, the most common "reader" of m6A and m6A-binding protein, can attenuate the inflammatory response and activate PTEN, and here we aimed to investigate its effect on epilepsy through epigenetics. All mice were injected intraperitoneally with 12 mg/kg of sea manic acid to establish an epilepsy model, and the epileptic behaviors of the mice were classified into 6 grades; epileptic behaviors of grade 3 or above were defined as seizures, and consecutive epileptic seizures of more than 30 min were considered as successful modeling. Mouse behavior was examined using the Morris Water Maze tracking assay; inflammatory factors IL-6, TNF-α, and IL-1β were detected by qPCR/WB/ELISA; cell activity was analyzed by CCK-8; apoptotic markers were identified by immunofluorescence assay and Western blot analysis. YTHDF1 knockout mice have poor spatial memory capacity and sensitivity to external stimuli. Under the influence of YTHDF1, the neuroinflammation and nseuron death decreased. YTHDF1 works by repressing the production of pro-inflammatory cytokines and the activation of astrocytes. It was found that YTHDF1 epigenetically activates PTEN through m6A modification, activates glial cells and represses pro-inflammatory cytokines production and inhibits the development of epilepsy.

1. Introduction

A frequent chronic neurological illness called epilepsy is brought on by an excess of neuronal discharges in the brain, which can induce seizures and other periodic abnormalities of the central nervous system [1,2]. Studies have reported that the incidence of epilepsy has reached 65 million cases worldwide, with a prevalence rate of more than 0.5 % [3]. The annual incidence of epilepsy in China is as high as 35.0/100,000, which has become the second largest category of neurological disorders [4,5]. It is characterized by recurrent seizures, the unpredictability of the duration of each seizure, and the long-term nature of drug treatment [6]. The etiology of epilepsy is diverse and can be broadly categorized as genetic [7], metabolic [8], structural, infectious [9], immunologic, and of unknown etiology.

N6-methyladenosine (m6A), the most common modification in mammalian mRNAs, also occurs in nucleosomal DNA and tRNAs,

* Corresponding author.
E-mail addresses: limingxia200506@163.com (M. Li), bzyjl1218@126.com (J. Yang), byytfyglx@bzmc.edu.cn (L. Gao).
[1] Mingxia Li and Junli Yang share first authorship.

https://doi.org/10.1016/j.heliyon.2024.e39481
Received 8 July 2024; Received in revised form 12 October 2024; Accepted 15 October 2024
Available online 17 October 2024

involving methylation at the N6 position [10]. m6A modification influences nearly all aspects of mRNA metabolism, including precursor mRNA splicing, mRNA transport from the nucleus, mRNA translation efficiency, as well as mRNA stability and subcellular localization [11]. YTH structural domain is the most common "reader" of m6A, and it is also the binding protein of m6A, acting through promoting the translation of m6A-modified mRNAs in the cytoplasm [12], YTHDF1 has been reported to play a major role in brain neurodevelopment, dopamine secretion and synapse formation mainly through binding to the m6A site of mRNAs [13], and is implicated to be linked with the occurrence, development and prognosis of various kind of diseases [14].

Phosphatase and tensin homolog deleted on chromosome ten (PTEN) is a novel tumor suppressor gene that was cloned in 1997 in the U.S.A. It is the first oncogene with dual-specificity phosphatase activity to be discovered to date [15]. PTEN regulates neuronal cell proliferation, migration, differentiation, and apoptosis. It exhibits high levels of expression in key brain areas, including the cerebellum, cerebral cortex, olfactory bulb, and hippocampus [16], along with other regions [17,18]. Furthermore, there is evidence to show that PTEN is crucial for the creation of synapses, and its absence in the brain is thought to alter synaptic transmission, structure, and plasticity [19]. Studies have indicated that the lack of the PTEN gene in the cortical and hippocampal neurons of fully developed mice leads to the occurrence of spontaneous seizures [20]. This highlights that research focusing on PTEN's role in neurological diseases is currently a trending area of interest.

2. Materials and methods

2.1. Reagents and biomolecules

In this study, a total of 54 adult male Wistar rats in good health weighing 180–250 g were used. Additionally, RT-PCR Reagents from Promega, USA, PTEN polyclonal antibody from Santa Cruz, USA, LPS from Sigma, USA, anti-GAPDH and secondary antibody from CST, USA, ELISA Kit from Elabscience, China, M6A Quantitative Measurement Kit from Elabscience, China, and BCA Protein Quantification Kit from Elabscience, China were utilised. The reference number for CTX-TNA2 from iCell was "Cell-r008." Four groups (sham group, KA group, KA + control group, and KA + YTHDF1 group) were randomly assigned to the modeled mice.

2.2. Role of YTHDF1 in epileptic mice

2.2.1. Western blot (WB) analysis of YTHDF1

After extracting the protein and preparing the protein prep gel, the extracted protein was sampled and subjected to electrophoresis. This was followed by the "sandwich" method of wet transfer for membrane transfer. After the membrane transfer, it was rinsed with 1 × TBST (Tris Buffered Saline Tween) for 5 min, three times. Following the TBST wash, the membrane was blocked with skim milk at room temperature for 1 h and kept at 4 °C overnight to incubate with the primary antibody. After 15 h, the membrane was incubated with the secondary antibody for 1 h, and then developing solution was added to the membrane. The total incubation period lasted around 15 h. Finally, the membrane was washed with TBST for 10 min each time.

2.2.2. Morris Water Maze tracking: behavioral test

The two primary components of the Morris Water Maze test program are the spatial exploration experiment and the localization navigation experiment. The five days of the localization navigation experiment, two for training and three for formal testing, were dedicated to determining the mice's escape latency. The formal test served as the basis for the statistical findings. The spatial exploration experiment lasted for one day and was conducted after the formal test of the localization navigation experiment. The pool was divided into four quadrants (I, II, III, and IV) based on the four entry points marked on the wall of the pool, with a hidden platform in quadrant III.

During the training period of the localization navigation experiment, the mice entered the water twice a day (six times a day) from the entry points in quadrants I, II, and IV. The image acquisition and processing system recorded the mice's trajectories, the time taken to find the hidden platform (i.e., escape latency), and other data. If the mice did not find the hidden platform within 60 s, the escape latency was recorded as 60 s, and the experimenters guided the mice to the platform. After the mice rested on the platform for 10 s, they were removed, and the next mouse was placed in the pool. During the formal test of the localization navigation experiment, the test was conducted in the same way as during the training period, and the data were collected. The spatial exploration experiment was conducted on the second day after the formal test. The steps for the mice entering the water remained unchanged, but the hidden platform in quadrant III was removed. The distance and time spent by the mice navigating in quadrant III were recorded to examine their memory of the original platform. The diameter of the swimming pool was 120 cm, the water depth was 30 cm, the hidden platform was 1–2 cm below the water surface, and the water temperature was maintained at 23 ± 1 °C.

2.2.3. qPCR/WB/ELISA analysis of IL-6, IL-1β, and TNF-α

Reverse transcription was done using a reverse transcription kit to create cDNA following the extraction of total RNA using the TRIZOL technique. A 10 μL reaction mixture containing 1 μL of cDNA, 0.5 μL of each upstream and downstream primer, 3.5 μL of DEPC water (diethypyrocarbonate-processed water), and 5 μL of 2 × SYBR mix was produced in accordance with the directions for the real-time quantitative PCR. The steps in the PCR reaction procedure were as follows: 30 s of pre-denaturation at 95 °C, 5 s of denaturation at 95 °C, and 30 s of extension at 60 °C. The degree of gene expression was measured after 40 cycles of the reaction, with β-actin acting as an internal reference.

The protein was extracted by adding RIPA protein lysate, quantified using the BCA method, electrophoresed, transferred to a

membrane, and blocked with 5 % BSA. IL-1β, IL-6, and TNF-α antibodies were added. The membrane was incubated overnight at 4 °C, followed by incubation with a peroxidase-labeled secondary antibody (1:5000 at PBS) at room temperature for 2.5 h the next day. After developing the color, pictures were taken, and the relative gray value of the bands was calculated using Image Pro Plus 6.0 software. Unless otherwise stated, thorough washing steps were carried out between each step. For the ELISA operation, the instruction manual of the ELISA kit and the product instruction manual were followed. A blank group, a standard group, and a sample group were set up. Accurately, 50 μL of standard samples were added to the enzyme-labeled coating plate. Sample dilution (40 μL) was added to the sample group, followed by the addition of 10 μL of the samples to be tested, and thoroughly mixed. To remove the tissue solution, the samples were incubated for 30 min at 37 °C, washed with detergent, and repeated five times. For each group, 50 μL of developer A and B were added and kept at 37 °C in the dark. After 10 min, the blank group was set to zero, and the absorbance of each group was measured at 450 nm (A). In each group, three samples were measured, and three tests were performed on each sample.

2.2.4. Nissl staining to analyze hippocampal neuronal damage in CA3, CAl, and Hilus areas

Paraffin sections were dewaxed to water, endogenous peroxidase was blocked with 3 % H2O2, and antigen retrieval was performed by heating with a water bath using sodium citrate buffer. The sections were then incubated in 5 % BSA for 2 h with a droplet of neutral dendritic gum. Rabbit anti-rat GFAP antibody (1:250, batch no. 80788) was added dropwise and incubated overnight at 4 °C. The following day, Alexa Fluor 488 labeled goat anti-rabbit secondary antibody (1:500, batch no. 4412) was added and incubated for 2 h. DAPI was used to stain the nuclei, and the slices were blocked and fixed. In the hippocampal CA3, CA1, and Hilus regions, 3 fields were randomly selected from each section and counted under high magnification (× 400).

2.2.5. Immunofluorescence/WB analysis of GFAP

Paraffin sections were routinely deparaffinized and hydrated. Antigen retrieval was performed using a hot repair method in a water bath, then the sections were cooled to room temperature and blocked with sealing solution for 90 min. The primary antibody, GFAP (diluted 1:500), was added and the sections were incubated overnight at 4 °C. The next day, the corresponding secondary antibody (diluted 1:500) was added and the sections were kept in the dark. The slices were sealed with an antifluorescence-quenching sealing agent containing DAPI. Fluorescence microscopy was used to observe and capture images. The expression of positive cells/vessels in the brain tissue around the infarct foci in the cortex on the ischemic side was observed and photographed under 200x and 400x microscope fields. Three locations of view were randomly selected under a 400x microscope for each sample. The total number of NF-κBp65 and the number of nuclei translocations in the brain tissue around the infarct foci were counted and analyzed using Image J software.

The protein was extracted by adding RIPA protein lysate, quantified using the BCA method, electrophoresed, transferred to a membrane, and blocked with 5 % BSA. An anti-GFAP antibody (1:500) was added, and the membrane was incubated overnight at 4 °C. The next day, a peroxidase-labeled anti-GFAP secondary antibody (1:5000) was added. After developing the color, photographs were taken, and the relative grayscale value of the bands was calculated using Image Pro Plus 6.0 software.

2.2.6. TUNEL analysis of apoptosis & WB analysis of apoptosis markers

According to the instructions of the TUNEL kit (Lot No. KGA7071-1), DAPI was used to stain the nuclei for 10 min and observed using a microscope. The images were analyzed using Image Pro Plus 6.0 software. Three different views were randomly taken in the CA3 region of the hippocampus in each section under high magnification (× 400), and the number of double-positive cells and the total number of cells were counted for MAP-2 and TUNEL, respectively. The apoptotic index was calculated as follows: apoptotic index = (number of double-positive cells/total number of cells) × 100 %. The average apoptotic index of three fields of view represented the neuronal apoptotic index of each rat.

The extracted protein concentration was determined using the BCA protein quantification kit, following the manufacturer's instructions. A 10 % SDS-PAGE gel was prepared, samples were loaded and electrophoresed, and the gel was subsequently transferred to a membrane. The membrane was incubated with 5 % skimmed milk powder under slow shaking conditions, followed by rinsing with TBST buffer (1 ×) for 10 min and washing three times. After cutting the membrane based on the molecular weight of each protein, primary antibodies (Bax, Bcl-2, Caspase-3, β-Actin at 1:1000 dilution) were added and incubated overnight at 4 °C. The membrane was then rinsed with TBST buffer and incubated with secondary antibody for 1 h at 37 °C with shaking, followed by washing with TBST for 30 min, three times. Finally, ECL chemiluminescent solution was applied for exposure and image capture. Image-J software was used to analyze the grayscale intensity of protein bands, calculate relative protein expression, and GraphPad Prism 8 software was employed to generate graphical representations.

2.3. Role of YTHDF1 in glial cells

2.3.1. Experimental grouping

Mice with successful modeling were divided into four groups: LPS group, control group, LPS + overexpression control null group, and LPS + YTHDF1 group.

2.3.2. CCK-8 analysis of cellular activity

Cell proliferation levels were assessed using the CCK-8 kit (Tokyo, Japan). Cells were detached with trypsin from 6-well plates, suspended, and seeded into 96-well plates for incubation. After stimulation with 0.5 μg/mL of LPS for 24 h at 37 °C, the cells were treated with CCK-8 reagent and incubated for 30 min. The absorbance (A) was then measured at 450 nm using a microplate reader

(BioTek, USA).

2.3.3. Flow cytometry analysis of apoptosis

After removing the supernatant, the cells were centrifuged for 5 min at 400×*g* at 4 °C and washed again with PBS. Annexin V-FITC and PI were then added and incubated for 30 min at 4 °C in the dark. Flow cytometry analysis will be performed immediately after cell incubation.

2.4. YTHDF1 epigenetically activates PTEN through m6A modification

2.4.1. Experimental grouping

The mice with successful modeling were divided randomly into two groups: control group, interfering YTHDF1 group.

2.4.2. qPCR analysis of PTEN

FLS were solubilized with TRIzol reagent to extract intact RNA. The TRIzol extract was separated with chloroform, centrifuged, and RNA was precipitated by adding isopropanol. After precipitation, the RNA pellet was washed with pre-cooled 75 % ethanol, centrifuged, and then dissolved in an appropriate amount of DEPC water. Reverse transcription was performed to obtain cDNA, followed by PCR amplification to detect mRNA expression. The experiment included 3 independent samples, with each sample analyzed in triplicate, and results were calculated using the 2-ΔΔCt method.

2.4.3. MeRIP-qPCR

To determine the quantity of m6A-changed Bcl-2 in cells, total RNA was extracted and purified using a PolyA mRNA purification kit. IP buffer was added to m6A and IgG antibodies, which were then incubated with protein A/G magnetic beads for 1 h to facilitate binding. Subsequently, the magnetic bead-antibody complexes and purified mRNA were incubated in IP buffer containing protease and ribonuclease inhibitors overnight at 4 °C. RNA was then extracted and purified using phenol-chloroform with elution buffer, followed by qPCR analysis of the results.

2.4.4. WB analysis of PTEN

To extract protein, RIPA protein lysate was added. Protein quantification was performed using the BCA method. Electrophoresis and membrane transfer were conducted, followed by blocking with 5 % BSA. The Bcl-2 antibody was applied at a 1:2000 dilution ratio and incubated overnight at 4 °C. The next day, a peroxidase-labeled secondary antibody was added and incubated at room temperature for 2.5 h. After developing the color and capturing images, the relative gray values of the bands were calculated using Image Pro Plus 6.0 software.

2.5. YTHDF1 acts through PTEN in epileptic mice

2.5.1. Experimental grouping

Successfully modeled mice were divided into six groups: sham group, KA group, KA + control group, KA + YTHDF1 group, KA + YTHDF1+shNC group and KA + YTHDF1+shPTEN group.

[1] 2.5.2. WB analysis of YTHDF1 and PTEN

[2] To extract protein, RIPA protein lysate was used. Protein quantification was performed using the BCA method. Electrophoresis and membrane transfer were conducted, followed by blocking with 5 % BSA. METTL3 and Bcl-2 antibodies were added simultaneously and incubated overnight at 4 °C. The following day, a peroxidase-labeled secondary antibody was applied and incubated at room temperature for 2.5 h. After developing the color and capturing images, the relative gray values of the bands were calculated using Image Pro Plus 6.0 software.

[3] 2.5.3. Detect YTHDF1 and PTEN and analyze the apoptosis markers with reference to the experimental method under "2.1".

2.6. YTHDF1 acts through PTEN in glial cells

2.6.1. Experimental grouping

Successfully modeled mice were divided into four groups: control group, LPS group, LPS + overexpression control null group, LPS + YTHDF1 group, YTHDF1+shNC group and LPS + YTHDF1+shPTEN group. Refer to the experiment under "2.2″ to study the role of YTHDF1 in glial cells through PTEN.

3. Results

3.1. YTHDF1 in epileptic mice

The results of the water maze experiments showed that, compared with the control group, the other three groups of mice had disorganized swimming trajectories and longer escape latencies during exploration. In addition, the mice swam significantly less distance, spent significantly less time, and crossed the escape platform in the target quadrant than the control group ($P < 0.05$). These

results (Fig. 1A and B) suggest that spatial exploration and learning memory abilities were significantly reduced in the other groups. In contrast, intervention with YTHDF1 significantly improved these abilities.

The relative mRNA levels of cytokines in the KA and KA + NC groups were significantly higher than those in the blank control group, as shown by qPCR and WB results (Fig. 1C and A). However, after the addition of YTHDF1, these levels returned to approximately the same level as the blank control group. ELISA results (Fig. 1C) showed that the cytokine concentrations in the other three groups were elevated compared with the blank control group. However, the addition of YTHDF1 resulted in a significant decrease ($P < 0.05$) in these concentrations, indicating a reduction in inflammatory factors. This suggests that YTHDF1 may regulate the development of epilepsy by modulating the expression levels of inflammatory factors.The results of Nissl staining (Fig. 1 D) showed that neurons in the hippocampal region of control mice were neatly aligned, with a high number of Nissl bodies, intact cellular structure, regular arrangement, and no obvious deletions. In contrast, the neurons in the KA and KA + NC groups of mice were significantly damaged ($P < 0.05$) and appeared disorganized and sparsely distributed. These groups also exhibited increased numbers of degenerated and necrotic cells and decreased Nissl bodies within neurons. However, intervention with YTHDF1 resulted in a significant increase in the number of Nissl bodies without significant morphological damage.

Immunofluorescence results (Fig. 1E and F) showed a significant increase ($P < 0.05$) in the number of fluorescent cells compared with the control group, indicating an increase in cell density under fluorescence microscopy. Western blot analysis of the astrocyte-specific marker GFAP showed (Fig. 1 E and G) a significant decrease ($P < 0.05$) in GFAP expression. TUNEL analysis of apoptosis (Fig. 1 F) showed a significantly higher rate of apoptosis compared to control ($P < 0.05$).

3.2. YTHDF1 in glial cells

The results of qPCR, WB and ELISA showed (Fig. 2A–C) that the relative mRNA levels and cytokine concentrations were significantly higher in the KA and KA + NC groups compared to the blank control group. However, the addition of YTHDF1 significantly reduced these concentrations ($P < 0.05$). CCK-8 and flow cytometry assays showed (Fig. 2 B and D) that the cell proliferation rate was significantly lower ($P < 0.05$) and apoptosis rate was increased ($P < 0.05$) compared with the control group. In contrast, under the influence of YTHDF1, the cell proliferation rate increased, and the apoptosis rate decreased. In addition, WB analysis of the astrocyte-specific marker GFAP (Fig. 2E and F) showed a significant decrease ($P < 0.05$), and the results of the analysis of apoptosis markers were consistent with the above findings.

3.3. YTHDF1 epigenetically activates PTEN through m6A modification

RNA and protein were extracted and analyzed by qRT-PCR, MeRIP-PCR, and Western blotting (Fig. 3A–C). PCR results showed that YTHDF1 significantly up-regulated the relative expression of HK2 mRNA compared with the control ($P < 0.05$). Western blot analysis (Fig. 3 D), which was consistent with the expression level of the internal reference protein, also showed that YTHDF1 significantly up-regulated HK2 mRNA ($P < 0.05$), and the up-regulation was reduced by inhibition of YTHDF1. Analysis of m6A using the M6A quantitative assay kit showed that YTHDF1 significantly increased the amount of M6A in mRNA compared with the control group ($P < 0.05$), and the amount decreased after inhibition of YTHDF1.

3.4. YTHDF1 acts through PTEN in epileptic mice

The results of the water maze experiment showed (Fig. 4A and B) that compared with the control group, the other three groups of mice had disorganized swimming trajectories and longer escape latency in the exploration phase. In addition, the swimming distance, time spent and the number of times these mice crossed the escape platform in the target quadrant were significantly lower than those of the control group ($P < 0.05$), indicating that the spatial exploratory ability and learning memory function of these mice were significantly reduced. However, the spatial exploration ability and learning memory function of mice were significantly improved after intervention with YTHDF1. qPCR and WB results showed (Fig. 4 A and C) that the relative mRNA levels of cytokines in the other groups were significantly higher than those in the blank control group. After the addition of YTHDF1, these levels were reduced to levels similar to those of the blank control group, but the mRNA levels were significantly increased after inhibition of PTEN expression ($P < 0.05$). ELISA results showed (Fig. 4C) that cytokine concentrations were elevated in the other three groups compared with the blank control group. However, these concentrations were significantly reduced after the addition of YTHDF1 ($P < 0.05$). Similarly, these concentrations changed significantly ($P < 0.05$) after inhibition of Bcl-2 expression, suggesting that YTHDF1 acts in epileptic mice by regulating PTEN.

After inhibition of PTEN expression, Nissl staining showed (Fig. 4 D) that neurons in the hippocampal region of mice transitioned from disorganized to aligned, with an increase in the number of Nissl bodies and an improvement in neuronal structure. Immunofluorescence analysis showed (Fig. 4 E) a significant decrease in the number of cells ($P < 0.05$), and Western blotting assay showed (Fig. 4F and G) a significant decrease in the astrocyte-specific marker GFAP ($P < 0.05$). TUNEL analysis of apoptosis showed (Fig. 4 F) that YTHDF1 significantly reduced apoptosis ($P < 0.05$). However, inhibition of PTEN expression significantly increased the apoptosis rate ($P < 0.05$).

3.5. YTHDF1 acts through PTEN in glial cells

The results of qPCR, WB, ELISA and CCK-8 with flow cytometry assays showed (Fig. 5A–C) that YTHDF1 significantly decreased the

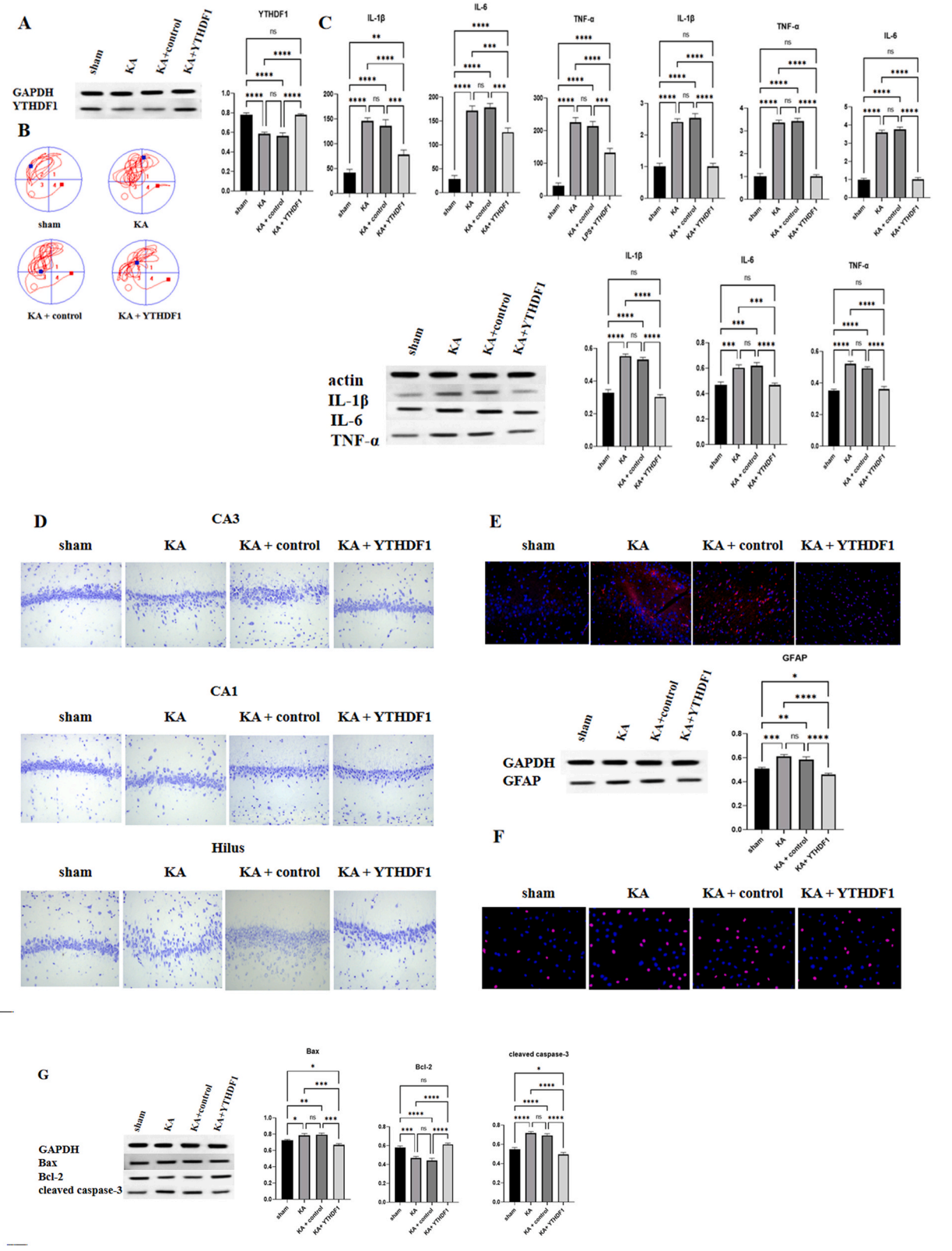

(caption on next page)

Fig. 1. YTHDF1 in Epileptic Mice. (A–G) WB analysis of METTL3 (A). Morris Water Maze tracking experiment (B). qPCR/WB/ELISA analysis of inflammatory factors TNF-α, IL-1β and IL-6 (C). Nissl staining analysis of hippocampal neuronal damage in CA3, CAl, and Hilus areas (D). Immunofluorescence/WB analysis of GFAP (E). TUNEL analysis of apoptosis, WB analysis of apoptosis markers (F and G). Uncropped images of original blotting are provided as supplementary file.

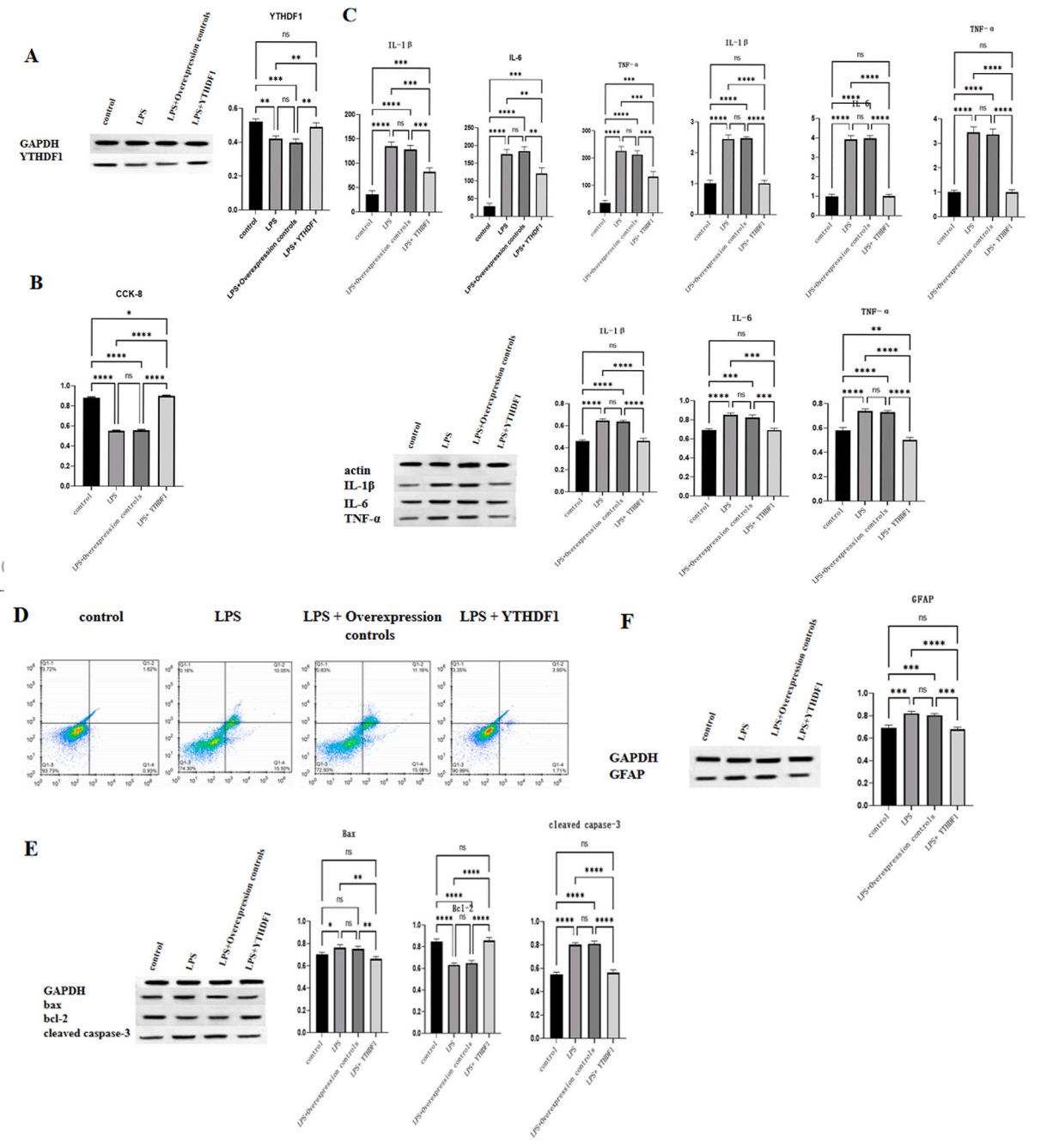

Fig. 2. YTHDF1 in glial cells. (A–F) WB analysis of METTL3 (A). qPCR/WB/ELISA analysis of inflammatory factors IL-6, IL-1β and TNF-α (B). CCK-8 analysis of cellular activity (C). Flow cytometry analysis of apoptosis (D). WB analysis of GFAP and apoptosis markers (E and F). Uncropped images of original blotting are provided as supplementary file.

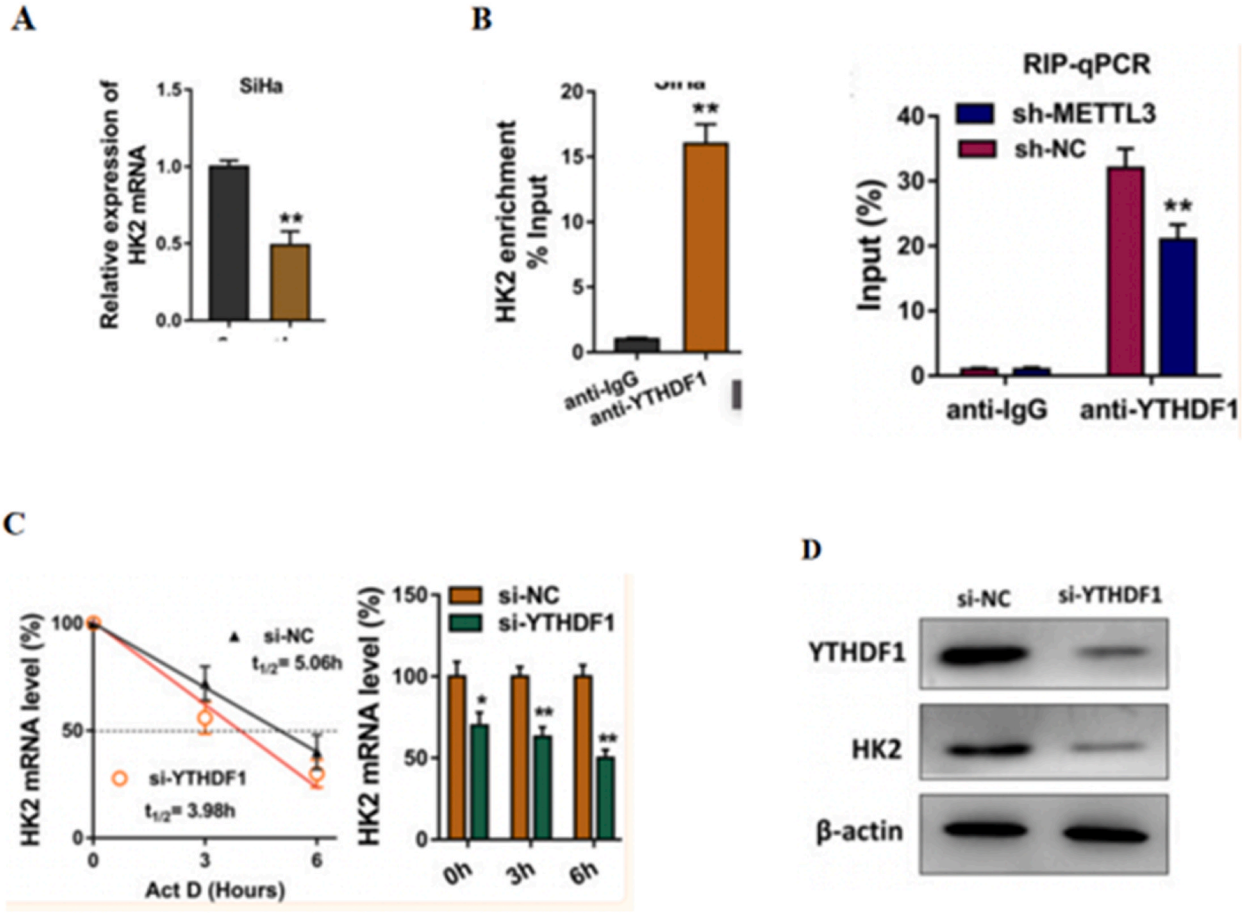

Fig. 3. YTHDF1 epigenetically activates PTEN through m6A modification. (A–D) qPCR analysis of Bcl-2 (A). Analysis of m6A was performed (B). MeRIP-qPCR analysis of METTL3 epigenetic activation of Bcl-2 by m6A modification (C). WB analysis of Bcl-2 (D). Uncropped images of original blotting are provided as supplementary file.

relative mRNA levels and concentrations of cytokines ($P < 0.05$), as well as significantly increased the rate of apoptosis ($P < 0.05$). In contrast, inhibition of PTEN expression resulted in a significant increase in cytokine concentration ($P < 0.05$) and a significant decrease in apoptosis rate ($P < 0.05$) (Fig. 5 D). The expression of the astrocyte-specific marker GFAP was assessed by WB (Fig. 5E and F), and apoptosis markers were also analyzed. the expression of GFAP was significantly decreased ($P < 0.05$) after YTHDF1 treatment, whereas the expression of GFAP was significantly increased ($P < 0.05$) after inhibition of PTEN expression.

4. Discussion

Epilepsy is a transient and sudden brain disorder characterized by excessive and repetitive discharges of neurons, leading to recurrent seizures. It is a prevalent neurological condition associated with high disability and mortality rates. Prolonged seizures in epilepsy can cause sustained damage to brain neurons, exacerbated by electrolyte disturbances, acid-base imbalances, and infections [21]. n6-methyladenosine (m6A) is the most prevalent modification in mammalian mRNAs, as well as in nucleoproteasomal DNA and tRNA. Catalyzed by the methyltransferase complex [22], and methyltransferases are core components, responsible for catalyzing the formation of m RNA m6A in eukaryotes. Mammalian YTHDF1 and hnRNP act as m6A recognition proteins to recognize and regulate the corresponding downstream molecular mechanisms [23,24]. YTHDF1 is a member of the family of proteins containing the YT521-B homologous structural domain. This protein recognizes m6A through its conserved aromatic group on the YTH structural domain, thereby mediating post-transcriptional gene regulation [25]. In the cytoplasm, YTHDF1 increases the delivery of mRNA transcription complexes by interacting with eIF3 and binding to the m6A site around the stop codon, uniting the translation initiation machinery to promote translation initiation and protein synthesis [26,27]. Other studies have also confirmed that YTHDF1 protein plays an important role in brain neurodevelopment, dopamine secretion and synapse formation, mainly through binding to the m6A site of mRNA [28]. In this study, authors performed Morris Water Maze tracking experiments and found that intervention with YTHDF1 significantly improved the spatial exploration ability and learning memory ability of mice; as Zhang et al. [29] first pointed out, the effect of m6A modification on the learning and memory ability of mice, YTDHF1 knockout mice have a spatial memory ability and

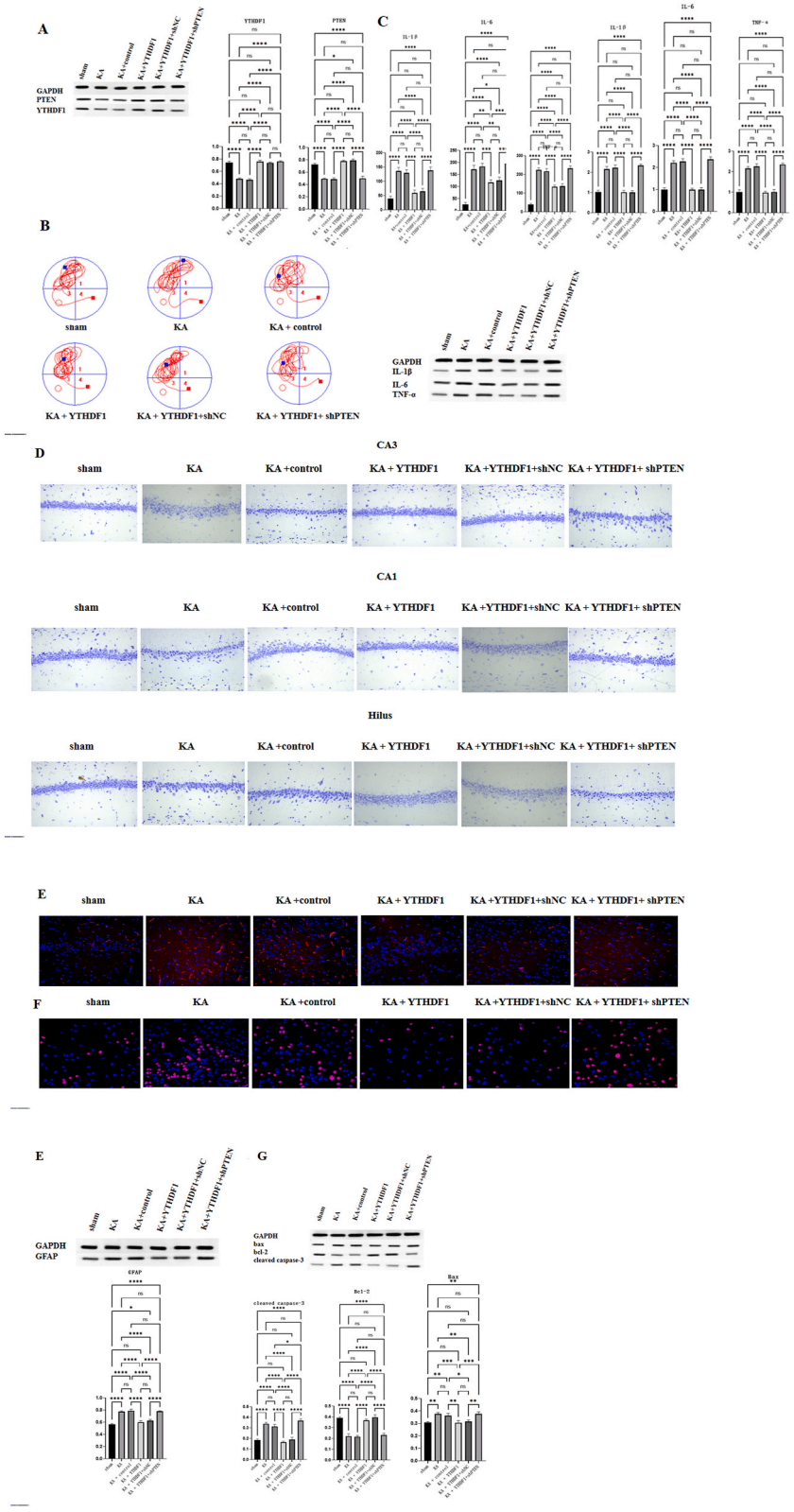

(caption on next page)

Fig. 4. YTHDF1 acts through PTEN in epileptic mice. (A–G) WB analysis of METTL3 and Bcl-2 (A). Morris Water Maze tracking experiment (B). qPCR/WB/ELISA analysis of inflammatory factors IL-6, IL-1β and TNF-α (C). Nissl staining to analyze hippocampal neuronal damage in CA3, CAl, and Hilus areas (D). Immunofluorescence/WB analysis of GFAP (E). TUNEL analysis of apoptosis, WB analysis of apoptosis markers (F and G). Uncropped images of original blotting are provided as supplementary file.

external stimulus sensitivity were poor. In our study we performed qPCR and WB, ELISA, Nissl staining, immunofluorescence and TUNEL to analyze apoptosis experiments. It was found that cytokine relative mRNA levels were restored to about the same level as the blank control group after the addition of YTHDF1; the concentration of inflammatory cytokines was significantly reduced ($P < 0.05$). In addition, after immunofluorescence and WB assay, it was found that with the participation of YTHDF1, the number of cells was significantly increased ($P < 0.05$), the GFAP was reduced significantly ($P < 0.05$) and the rate of apoptosis was reduced significantly ($P < 0.05$). It proved that YTHDF1 could inhibit the development of epilepsy.

Inflammatory dysregulation has been found to be a pathological feature of central nervous system (CNS) disorders, including epilepsy [30]. Furthermore, one of the main cell types implicated in neuroinflammation—which is crucial to the etiology and advancement of neurodegenerative diseases—is mouse microglia, or BV-2 cells.By deactivating the PI3K/Akt signalling pathway, Ji JW [31]et al. discovered that Mettl3 plays a vital role in the growth, invasion and migration glioma cells. This finding offers a novel mechanism for neuroglial carcinogenesis and suggests a new target for the therapy of neuroglial tumors. A novel mechanism for the carcinogenesis of gliomas and offers fresh opportunities for glioma treatment. Therefore, we explored the role of YTHDF1 in glial cells experimentally. qPCR, WB and ELISA results showed that the concentration of inflammatory cytokines and relative mRNA levels were significantly reduced by the addition of YTHDF1 ($P < 0.05$). CCK-8 and flow assay results showed that cellular value-added rate was increased, and apoptosis was decreased by the effect of YTHDF1. The expression of astrocyte-specific marker GFAP was detected by WB and apoptosis markers were analyzed, and the results showed that GFAP was significantly reduced ($P < 0.05$). It was demonstrated that YTHDF1 inactivated astrocytes and repressed the release of pro-inflammatory cytokines.

The chromosome 10 homologous lost phosphatase tension protein gene, PTEN, is a highly conserved oncogene with dual-specificity phosphatase activity with 99.75 % homology in human, mouse and dog, discovered in 1997 [32]. The PTEN gene has attracted much attention since its discovery, and the encoded protein negatively regulates the PI3K/AKT signaling pathway by catalyzing the dephosphorylation of phosphatidylinositol triphosphate (PTP) to phosphatidylinositol diphosphate (PDP), which is a gene closely related to the development of multiple tumors after P53 [33]. Currently, the study of PTEN has been expanded from tumor cells to neuronal cells, cardiomyocytes, smooth muscle cells, etc., and the related diseases have been expanded from cancer to neurological diseases, heart failure, atherosclerosis, etc., and the use of PTEN in the study of neurological diseases is the hotspot of the current stage. According to recent research, PTEN is extensively involved in the regulation of neuronal proliferation, migration, differentiation, apoptosis, and synapse establishment, all of which are critical for neuronal growth. It is highly expressed in the cerebral cortex, cerebellum, hippocampus, and olfactory bulb [34,35].

Mutations in the PTEN gene are highly linked in the phenotypic abnormalities range, and manifested in the nervous system such as macrocephaly [36], epilepsy [37,38], ataxia, intellectual disability, and autism [39,40]. In our experiments, inhibiting the expression of YTHDF1 significantly reduced HK2 mRNA expression and M6A modification in mRNA ($P < 0.05$). Conversely, inhibiting the expression of PTEN in mice resulted in a significant decrease in spatial exploration and learning memory abilities, accompanied by a significant increase in mRNA levels ($P < 0.05$) and concentrations of inflammatory factors ($P < 0.05$). Nissl staining revealed disorganized and sparsely distributed neurons in the hippocampal region, with an increase in degenerated and necrotic cells. TUNEL analysis showed a significant increase in apoptosis rate ($P < 0.05$). These findings suggest that YTHDF1 plays a crucial role in epilepsy development by epigenetically activating PTEN through m6A modification. Furthermore, inhibiting PTEN expression significantly decreased the apoptosis rate ($P < 0.05$) as determined by CCK-8 with flow cytometry assays. This implies that YTHDF1 activates glial cells, prompting them to release pro-inflammatory cytokines via PTEN activation, thereby inhibiting epilepsy development. In summary, our study demonstrates that YTHDF1 inhibits apoptosis and repressed pro-inflammatory cytokine release through glial cell activation. Further investigations support that YTHDF1 suppresses epileptic disease progression via PTEN activation towards the modern application [41].

CRediT authorship contribution statement

Mingxia Li: Writing – original draft, Methodology, Investigation. **Junli Yang:** Validation, Software, Investigation. **Lixiang Gao:** Writing – review & editing, Supervision, Conceptualization.

Ethical approval

The laboratory animal welfare and Ethical committee (Yantai Affiliated Hospital of Binzhou Medical University) approved this project: MDL2022-12-05-01.

Data and code availability

No data was used for the research described in the article.

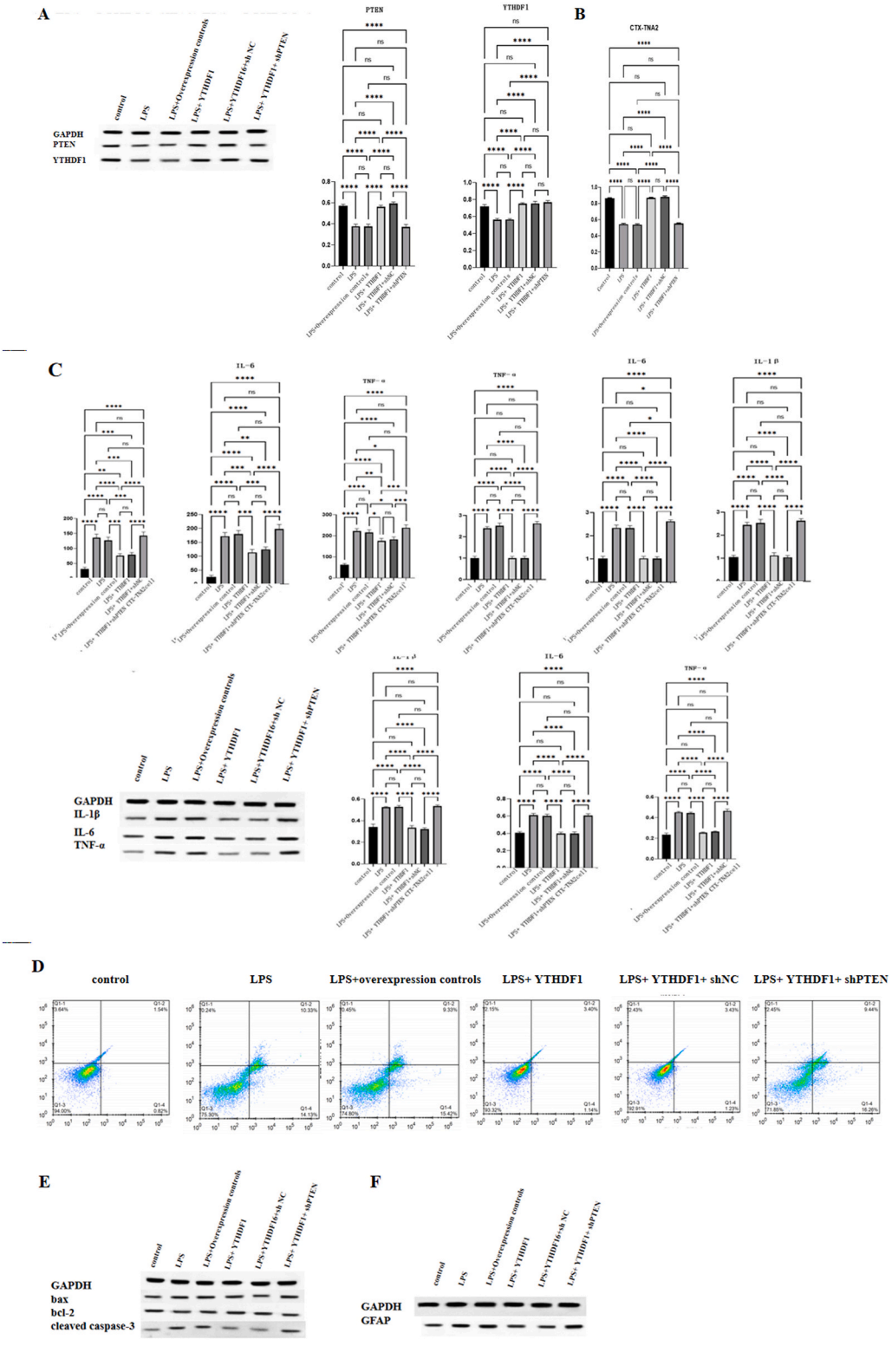

Fig. 5. YTHDF1 acts through PTEN in glial cells. (A–F) WB analysis of METTL3 and Bcl-2 (A). CCK-8 analysis of cellular activity (B). qPCR/WB/ELISA analysis of inflammatory factors IL-1β, TNF-α and IL-6 (C). Flow cytometry analysis of apoptosis (D) WB analysis of GFAP and markers of apoptosis. (E and F). Uncropped images of original blotting are provided as supplementary file.

Declaration of competing interest

The authors declare that they have no known competing financial interests or personal relationships that could have appeared to influence the work reported in this paper.

Appendix A. Supplementary data

Supplementary data to this article can be found online at https://doi.org/10.1016/j.heliyon.2024.e39481.

References

[1] E. Beghi, The epidemiology of epilepsy, Neuroepidemiology 54 (2) (2020) 185–191.
[2] J.D. Thurman, E.C. Begley, A. Carpio, et al., Primary prevention of epilepsy: a report from the international league against epilepsy prevention working group, J. Epilepsy 5 (6) (2019) 467–474.
[3] N. Freidel, L. Kreuder, B.S. Rabinovitch, F.Y. Chen, R.S.T. Huang, E.C. Lewis, Psychedelics, epilepsy, and seizures: a review, Front. Pharmacol. 14 (2024) 1326815.
[4] J. Falco-Walter, Epilepsy-definition, classification, pathophysiology, and epidemiology, Semin. Neurol. 40 (6) (2020 Dec) 617–623.
[5] E. Akyuz, A.K. Polat, E. Eroglu, et al., Revisiting the role of neurotransmitters in epilepsy: an updated review, Life Sci. 265 (2021) 118826.
[6] M. Leonardi, P. Martelletti, R. Burstein, et al., The world health organization intersectoral global action plan on epilepsy and other neurological disorders and the headache revolution: from headache burden to a global action plan for headache disorders, J. Headache Pain 25 (1) (2024 Jan 4) 4.
[7] K. Hundallah, B. Tabarki, Treatable inherited metabolic epilepsies, Neurosciences 26 (3) (2021) 229–235.
[8] B. Tumiene, C.R. Ferreira, C.D.M. van Karnebeek, Overview of metabolic epilepsies, Genes 13 (3) (2022) 508 (Basel). 2022 Mar 12.
[9] C.H. Lin, Y.T. Lu, C.J. Ho, et al., The different clinical features between autoimmune and infectious status epilepticus, Front. Neurol. 10 (2019 Feb 13) 25.
[10] X. Zhang, R.M. Blumenthal, X. Cheng, A role for N6-methyladenine in DNA damage repair, Trends Biochem. Sci. 46 (3) (2021 Mar) 175–183.
[11] H. Yang, Y. Li, L. Huang, et al., The epigenetic regulation of RNA N6-methyladenosine methylation in glycolipid metabolism, Biomolecules 13 (2) (2023 Feb 1) 273.
[12] E. Orouji, W.K. Peitsch, A. Orouji, et al., Oncogenic role of an epigenetic reader of m6A RNA modification: YTHDF1 in merkel cell carcinoma, Cancers 12 (1) (2020 Jan 14) 202.
[13] X. Zhao, Y. Chen, Q. Mao, et al., Overexpression of YTHDF1 is associated with poor prognosis in patients with hepatocellular carcinoma, Cancer Biomark 21 (4) (2018) 859–868.
[14] S. Wu, Y. Ai, H. Huang, et al., A synthesized olean-28,13β-lactam targets YTHDF1-GLS1 axis to induce ROS-dependent metabolic crisis and cell death in pancreatic adenocarcinoma, Cancer Cell Int. 22 (1) (2022 Apr 2) 143.
[15] J. Zhang, Y. Zhang, X. Lin, et al., The effects of the tumor suppressor gene *PTEN* on the proliferation and apoptosis of breast cancer cells via AKT phosphorylation, Transl. Cancer Res. 12 (7) (2023 Jul 31) 1863–1872.
[16] S. Yin, Y. Meng, C. Liu, Y. Wang, MIUH inhibits the hippocampal neuron growth in fetal rat by affecting the PTEN pathway, Neurochem. Res. 46 (8) (2021 Aug) 2046–2055.
[17] Y. Luan, H. Zhang, K. Ma, et al., CCN3/NOV regulates proliferation and neuronal differentiation in mouse hippocampal neural stem cells via the activation of the notch/PTEN/AKT pathway, Int. J. Mol. Sci. 24 (12) (2023 Jun 19) 10324.
[18] C. Guan, L. Luan, J. Li, L. Yang, MiR-212-3p improves rat functional recovery and inhibits neurocyte apoptosis in spinal cord injury models via PTEN downregulation-mediated activation of AKT/mTOR pathway, Brain Res. 1768 (2021 Oct 1) 147576.
[19] E.R. Cullen, K. Tariq, A.N. Shore, et al., mTORC2 inhibition improves morphological effects of PTEN loss, but does not correct synaptic dysfunction or prevent seizures, J. Neurosci. 43 (5) (2023 Feb 1) 827–845.
[20] A.R. White, D. Tiwari, M.C. MacLeod, et al., PI3K isoform-selective inhibition in neuron-specific PTEN-deficient mice rescues molecular defects and reduces epilepsy-associated phenotypes, Neurobiol. Dis. 144 (2020 Oct) 105026.
[21] W. Löscher, H. Potschka, S.M. Sisodiya, et al., Drug resistance in epilepsy: clinical impact, potential mechanisms, and new innovative treatment options, Pharmacol. Rev. 72 (3) (2020 Jul) 606–638.
[22] H. Yang, Y. Li, L. Huang, et al., The epigenetic regulation of RNA N6-methyladenosine methylation in glycolipid metabolism, Biomolecules 13 (2) (2023 Feb 1) 273.
[23] J. Li, K. Chen, X. Dong, et al., YTHDF1 promotes mRNA degradation via YTHDF1-AGO2 interaction and phase separation, Cell Prolif. 55 (1) (2022 Jan) e13157.
[24] J. Li, K. Chen, X. Dong, et al., YTHDF1 promotes mRNA degradation via YTHDF1-AGO2 interaction and phase separation, Cell Prolif. 55 (1) (2022 Jan) e13157.
[25] D.J. Kim, A. Iwasaki, YTHDF1 control of dendritic cell cross-priming as a possible target of cancer immunotherapy, Biochemistry 58 (15) (2019 Apr 16) 1945–1946.
[26] R. Anita, A. Paramasivam, J.V. Priyadharsini, et al., The m6A readers *YTHDF1* and *YTHDF3* aberrations associated with metastasis and predict poor prognosis in breast cancer patients, Am. J. Cancer Res. 10 (8) (2020 Aug 1) 2546–2554.
[27] S. Liu, G. Li, Q. Li, et al., The roles and mechanisms of YTH domain-containing proteins in cancer development and progression, Am. J. Cancer Res. 10 (4) (2020 Apr 1) 1068–1084.
[28] J.T. Roberts, A.M. Porman, A.M. Johnson, Identification of m6A residues at single-nucleotide resolution using eCLIP and an accessible custom analysis pipeline, RNA 27 (4) (2021 Apr) 527–541.
[29] Z. Zhang, K. Luo, Z. Zou, et al., Genetic analyses support the contribution of mRNA N6-methyladenosine (m6A) modification to human disease heritability, Nat. Genet. 52 (9) (2020 Sep) 939–949.
[30] L.B. Bergantin, The interplay among epilepsy, Parkinson's disease and inflammation: revisiting the link through Ca2+/cAMP signalling, Curr Neurovasc Res 18 (1) (2021) 162–168.
[31] J.W. Ji, Y.D. Zhang, Y.J. Lai, et al., Mettl3 regulates the proliferation, migration and invasion of glioma cells by inhibiting PI3K/Akt signaling pathway, Eur. Rev. Med. Pharmacol. Sci. 24 (7) (2020 Apr) 3818–3828.
[32] Q. Hao, S.M. Henning, C.E. Magyar, et al., Enhanced chemoprevention of prostate cancer by combining arctigenin with green tea and quercetin in prostate-specific phosphatase and tensin homolog knockout mice, Biomolecules 14 (1) (2024 Jan 14) 105.
[33] D. Ren, Y. Sun, D. Li, H. Wu, X. Jin, USP22-mediated deubiquitination of PTEN inhibits pancreatic cancer progression by inducing p21 expression, Mol. Oncol. 16 (5) (2022 Mar) 1200–1217.
[34] K. Tariq, E. Cullen, S.A. Getz, et al., Disruption of mTORC1 rescues neuronal overgrowth and synapse function dysregulated by Pten loss, Cell Rep. 41 (5) (2022 Nov 1) 111574.
[35] S. Meyer Zu Reckendorf, D. Moser, A. Blechschmidt, et al., Motoneuron-specific PTEN deletion in mice induces neuronal hypertrophy and also regeneration after facial nerve injury, J. Neurosci. 42 (12) (2022 Mar 23) 2474–2491.

[36] S. Fu, L.A.D. Bury, J. Eum, et al., Autism-specific PTEN p.Ile135Leu variant and an autism genetic background combine to dysregulate cortical neurogenesis, Am. J. Hum. Genet. 110 (5) (2023 May 4) 826–845.
[37] C. Franquelim, A. Romana, A. Rachão, et al., Early-onset dystonia and visual impairment preceding epileptic encephalopathy associated with PIGA gene mutation, Neuropediatrics 55 (4) (2024 Aug 2) 265–268.
[38] A.A. Asadi-Pooya, Precision medicine in epilepsy management; GET application (gene, epilepsy, treatment), Clin. Neuropharmacol. 46 (3) (2023 May-Jun 01) 95–97.
[39] S. Fu, L.A.D. Bury, J. Eum, A. Wynshaw-Boris, Autism-specific PTEN p.Ile135Leu variant and an autism genetic background combine to dysregulate cortical neurogenesis, Am. J. Hum. Genet. 110 (5) (2023 May 4) 826–845.
[40] N. Wu, X. Zhang, Y. Wang, Vertigo or dizziness as the first presentation of epilepsy: a case report, Adv Neurology 1 (3) (2022), https://doi.org/10.36922/an.v1i3.140.
[41] Q. Yu, Y. Jiao, R. Huo, H. Xu, J. Wang, S. Zhao, Q. He, J. Zhang, Y. Sun, S. Wang, J. Zhao, Y. Cao, Application of the concept of neural networks surgery in cerebrovascular disease treatment, Brain & Heart 1 (1) (2022) 223, https://doi.org/10.36922/bh.v1i1.223.